SRK signaling. The plasma membrane localization of MLPK suggests that it may function in the vicinity of SRK. In animal cells, members of the membrane-anchored Src family of protein tyrosine kinases interact with activated receptor tyrosine kinases and mutually stimulate each other's catalytic activity, thereby strengthening and prolonging the signal (*27*). MLPK, acting within the SRK receptor complex, is an attractive model for the future study of SI signaling.

References and Notes

1. A. G. McCubbin, T.-H. Kao, *Annu. Rev. Cell Dev. Biol.* **16**, 333 (2000).
2. J. C. Stein, B. Howlett, D. C. Boyes, M. E. Nasrallah, J. B. Nasrallah, *Proc. Natl. Acad. Sci. U.S.A.* **88**, 8816 (1991).
3. T. Takasaki *et al*., *Nature* **403**, 913 (2000).
4. G. Suzuki *et al*., *Genetics* **153**, 391 (1999).
5. S. Takayama *et al*., *Proc. Natl. Acad. Sci. U.S.A.* **97**, 1920 (2000).
6. C. R. Schopfer, M. E. Nasrallah, J. B. Nasrallah, *Science* **286**, 1697 (1999).
7. S. Takayama *et al*., *Nature* **413**, 534 (2001).
8. A. Kachroo, C. R. Schopfer, M. E. Nasrallah, J. B. Nasrallah, *Science* **293**, 1824 (2001).
9. T. Gu, M. Mazzurco, W. Sulaman, D. D. Matias, D. R. Goring, *Proc. Natl. Acad. Sci. U.S.A.* **95**, 382 (1998).
10. S. L. Stone, E. M. Anderson, R. T. Mullen, D. R. Goring, *Plant Cell* **15**, 885 (2003).
11. S. L. Stone, M. Arnoldo, D. R. Goring, *Science* **286**, 1729 (1999).
12. K. Hinata, K. Okazaki, T. Nishio, in *Proceedings of the 6th International Rapeseed Conference*, Paris, 17 to 19 May 1983 (Groupe Consultatif International de Recherche sur le Colza), vol. 1, pp. 354–359.
13. S. Ikeda, J. B. Nasrallah, R. Dixit, S. Preiss, M. E. Nasrallah, *Science* **276**, 1564 (1997).
14. M. Marin-Olivier, T. Chevalier, I. Fobis-Loisy, C. Dumas, T. Gaude, *Plant J.* **24**, 231 (2000).
15. E. Fukai, T. Nishio, M. E. Nasrallah, *Mol. Genet. Genomics* **265**, 519 (2001).
16. Materials and methods are available as supporting material on *Science* Online.
17. H. Shiba *et al*., *Biosci. Biotechnol. Biochem.* **67**, 622 (2003).
18. G. A. Thompson Jr., H. Okuyama, *Prog. Lipid Res.* **39**, 19 (2000).
19. S. Hanks, A. M. Quinn, *Methods Enzymol.* **200**, 38 (1991).
20. S.-H. Shiu, A. B. Bleecker, *Proc. Natl. Acad. Sci. U.S.A.* **98**, 10763 (2001).
21. T. Hirayama, A. Oka, *Plant Mol. Biol.* **20**, 653 (1992).
22. K. Murase *et al*., unpublished data.
23. Y. Miyake, S. Tajima, T. Funahashi, T. Yamamura, A. Yamamoto, *Eur. J. Biochem.* **210**, 1 (1992).
24. N. Martin *et al*., *Nat. Genet.* **32**, 443 (2002).
25. K. U. Torii, *Curr. Opin. Plant Biol.* **3**, 361 (2000).
26. S. Takayama, Y. Sakagami, *Curr. Opin. Plant Biol.* **5**, 382 (2002).
27. S. M. Thomas, J. S. Brugge, *Annu. Rev. Cell Dev. Biol.* **13**, 513 (1997).

28. We thank K. Hinata for advice and providing plant materials, H. Etoh for advice and help, Y. Okumoto for γ irradiation, A. Miyawaki for providing GFP vector, K. Kato for providing tobacco BY-2 cells, T. Entani and H. Shimosato for discussions, and T. Ueda and H. Sugita for technical assistance. This work was partly supported by Grants-in-Aid for Scientific Research [number (no.) 14360066 to S.T. and no. 11238205 and no. 15208013 to A.I.] from the Ministry of Education, Sports, Science, and Technology (MEXT) of Japan, by grant no. RFTF 00L01605 (to S.T.) from the Japan Society for the Promotion of Science, and by the MEXT Grant-in-Aid for the 21st Century Centers of Excellence (COE) Program to Nara Institute of Science and Technology.

Supporting Online Material

www.sciencemag.org/cgi/content/full/303/5663/1516/DC1
Materials and Methods
Fig. S1
References

12 November 2003; accepted 6 January 2004

A Kinesin-like Motor Inhibits Microtubule Dynamic Instability

Henrik Bringmann,[1]* Georgios Skiniotis,[2]† Annina Spilker,[1]‡ Stefanie Kandels-Lewis,[1] Isabelle Vernos,[1] Thomas Surrey[1]§

The motility of molecular motors and the dynamic instability of microtubules are key dynamic processes for mitotic spindle assembly and function. We report here that one of the mitotic kinesins that localizes to chromosomes, Xklp1 from *Xenopus laevis*, could inhibit microtubule growth and shrinkage. This effect appeared to be mediated by a structural change in the microtubule lattice. We also found that Xklp1 could act as a fast, nonprocessive, plus end–directed molecular motor. The integration of the two properties, motility and inhibition of microtubule dynamics, in one molecule emphasizes the versatile properties of kinesin family members.

The activities of a variety of molecular motors are required to spatially organize microtubules and chromosomes in the mitotic spindle (*1*, *2*). Some motors contribute to spindle pole focusing (*3*, *4*), others stabilize antiparallel microtubule overlaps in the spindle midzone (*5*), and yet others are involved in chromosome-microtubule interactions (*6–8*). How these different functions depend on the characteristics of the motors' kinetic behavior is unclear. Local and temporal modulation of microtubule dynamics by stabilizing and destabilizing factors is also necessary for spindle assembly and function (*9–14*).

Little is known about the interaction between microtubules and chromosome arms that are covered with chromokinesins. One of these kinesins is *Xenopus laevis* kinesin-like protein 1 (Xklp1), a member of the Kif4 subfamily. Xklp1 is important for chromosome-microtubule interactions and for spindle pole extension (*4*, *7*). Its C-terminal part

[1]Cell Biology and Biophysics Programme, and [2]Structural and Computational Programme, European Molecular Biology Laboratory, Meyerhofstraβe 1, 69117 Heidelberg, Germany.

*Present address: Max Planck Institute of Molecular Cell Biology and Genetics, Pfotenhauerstraβe 108, 01307 Dresden, Germany.
†Present address: Department of Cell Biology, Harvard Medical School, Boston, MA 02115, USA.
‡Present address: Institute of Biochemistry, ETH Hoenggerberg, 8093 Zürich, Switzerland.
§To whom correspondence should be addressed. E-mail: surrey@embl.de

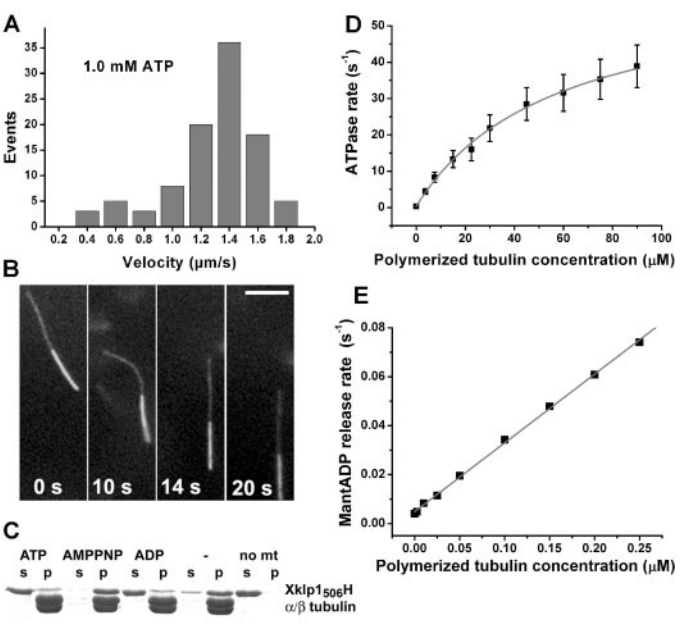

Fig. 1. Kinetics of Xklp1. (**A**) Histogram of the velocity of microtubule gliding generated by $Xklp1_{507}GST$ at 1 mM ATP. (**B**) A polarity-marked microtubule moving in a gliding assay with 0.1 mM ATP on a $Xklp1_{507}GST$ covered surface with its brightly labeled minus end–leading. Twenty-four out of 25 polarity-marked microtubules with clearly recognizable polarity showed this plus end–directed motility. Bar, 5 μm. (**C**) Coomassie-stained SDS gel of a microtubule copelleting assay. p, pellet; s, supernatant; no mt, without microtubules; –, without additional nucleotide. All Xklp1 constructs showed comparable results (data shown here for $Xklp1_{506}H$, see also Fig. S3). (**D**) Microtubule-stimulated steady state ATPase rate of $Xklp1_{506}H$ measured using an enzyme-linked assay (*24*). (**E**) Rate of productive encounters. The pre–steady state parameter k_{bi} was determined by measuring the release of the fluorescent ADP analog mant-ADP from nucleotide-preloaded motor after its binding to microtubules (*21*). The linear increase of the release rate with the microtubule concentration (at subsaturating microtubule concentrations) provides the second-order rate constant k_{bi}. The unusually low k_{bi} of Xklp1 accounts for the high $K_{0.5MT}$.

targets the molecule to chromosomes (*15*), but the molecular mechanism of the interaction of the N-terminal motor domain with microtubules is not understood. To gain insight into the basic characteristics of this kinesin-like protein, we examined the kinetic properties of the putative motor domain of Xklp1 and its influence on microtubule dynamics in vitro.

A purified fusion protein consisting of the predicted N-terminal motor domain and part of the coiled coil of Xklp1 and a C-terminal glutathione *S*-transferase (GST) tag ($Xklp1_{507}GST$) was tested for motility in gliding assays (*16*–*18*). Microtubule gliding was observed, and the velocity distribution peaked around 1.4 μm/s in the presence of 1 mM adenosine triphosphate (ATP) (Fig. 1A). Xklp1 was a plus end–directed motor (Fig. 1 B), like the homologous mouse Kif4 (*19*). In contrast to Kif4, however, Xklp1 acted as a fast molecular motor.

To characterize the processivity of Xklp1, a construct with a C-terminal His_6-tag ($Xklp1_{506}H$) was used. $Xklp1_{506}H$ was in its dimeric, native state (*4*, *16*) (fig. S1). The chemical processivity, i.e., the number of ATP molecules hydrolyzed per productive encounter of the motor with a microtubule (*20*), was determined by steady state and pre–steady state kinetic measurements (Fig. 1, D and E) (*16*). A fast steady-state adenosine triphosphatase (ATPase) turnover rate k_{cat} of 62 ± 17 s^{-1} and a Michaelis-Menten constant $K_{0.5MT}$ of 58 ± 29 μM (Fig. 1D) were obtained. The $K_{0.5MT}$ was two orders of magnitude higher than that of other motile kinesins (*20*–*22*) and indicated very weak microtubule binding of the motor in the presence of ATP. The ratio of $k_{cat}/K_{0.5MT}$ of about 1.1 $\mu M^{-1}s^{-1}$ is in the order of magnitude expected for a diffusion-limited reaction of a kinesin (*23*) and does not suggest a processive mechanism of ATP hydrolysis (*24*). The nonprocessive nature of Xklp1 activity was confirmed by measuring the bimolecular rate of productive encounters k_{bi} of 0.28 ± 0.01 $\mu M^{-1}s^{-1}$ under pre–steady state conditions (*16*, *20*, *25*) (Fig. 1E). Because this value is quite low for a kinesin (*21*, *22*) and comparable to the apparent bimolecular rate $k_{cat}/K_{0.5MT}$, it can be concluded that $Xklp1_{506}H$ is nonprocessive or at most weakly processive (*20*).

Although $Xklp1_{506}H$ showed adenine nucleotide–dependent binding to paclitaxel-stabilized microtubules typical for kinesins (Fig. 1C), its fast motility and its very weak binding to microtubules when ATP was present are more reminiscent of myosin II than of other kinesins (*26*, *27*). Xklp1 probably acts as a "rower" (*28*) and may only generate efficient movement in large assemblies, e.g., on chromosomes (similar to myosin II, which assembles into large arrays in myosin fibers).

We then tested whether Xklp1 affected microtubule dynamics. $Xklp1_{506}H$ was added to pregrown microtubule asters nucleated from centrosomes, and the dynamics of individual microtubules in the presence of 30 μM tubulin, 1 mM GTP, and 1 mM ATP were observed by video-enhanced differential interference contrast (DIC) microscopy (*12*, *16*). Under these conditions, most microtubules were growing. The speed of microtubule polymerization was slowed down with increasing motor concentration and was completely inhibited above a concentration of 10 μM of $Xklp1_{506}H$ motor domains, resulting in static microtubules (Fig. 2A; fig. S2). Washing out the motor restored microtubule polymerization, showing the reversibility of this effect. Experiments in which the motor was not washed out indicated a limited stability of static microtubules at higher motor concentrations on a slower time scale. Whereas static microtubules were still present after 20 min in the presence of 10 μM $Xklp1_{506}H$, half of the microtubules had disappeared after 5 min with 25 μM motor.

Next, we examined the effect of Xklp1 on shrinking microtubules. Microtubules were first grown from centrosomes with $Xklp1_{506}H$ concentrations that were only weakly growth-inhibiting. Keeping the motor concentration constant, tubulin and GTP were then washed out to induce microtubule depolymerization. $Xklp1_{506}H$ slowed down microtubule depolymerization with increasing motor concentration (Fig. 2B; fig. S2). It completely inhibited microtubule shrinking at motor concentrations around 1 μM of $Xklp1_{506}H$ motor domains. Because essentially no free tubulin was present during depolymerization, Xklp1's effect must have been due to an interaction with the microtubule, not with free tubulin. Microtubules grown from axonemes showed that inhibition of microtubule dynamics was not restricted to microtubule plus ends. Thus, Xklp1 was able to fully inhibit both microtubule polymerization as well as depolymerization.

To learn more about the mechanism of Xklp1-mediated inhibition of microtubule dynamics, its nucleotide dependence was examined. Asters were nucleated from centrosomes in the presence of $Xklp1_{506}H$ and different adenine nucleotides. They were fixed at defined time points before they had

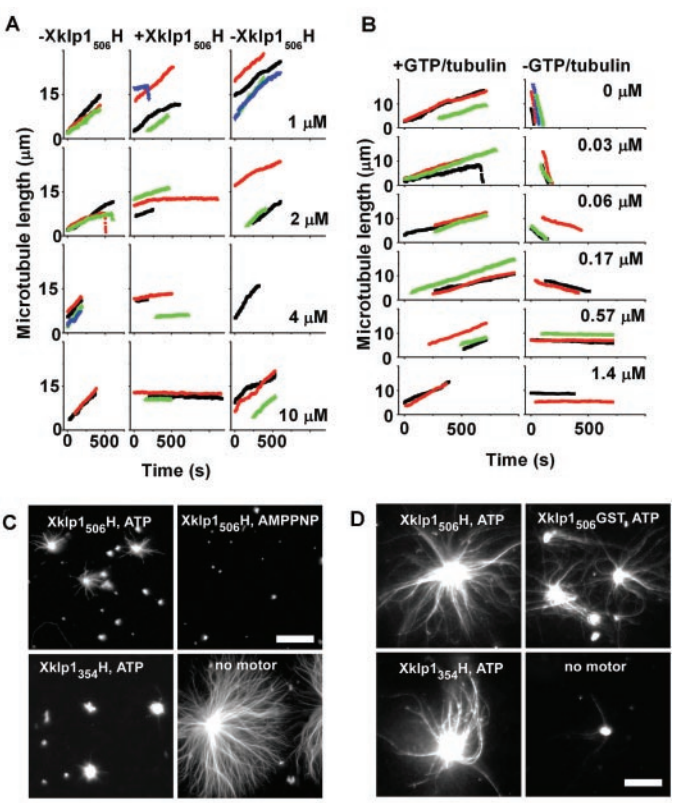

Fig. 2. Xklp1 is an inhibitor of microtubule dynamics: (**A** and **B**) Dynamic microtubule asters nucleated from centrosomes were visualized by DIC microscopy and the length of individual microtubules was plotted versus time. (A) Concentration-dependent and reversible inhibition of microtubule growth. Four experiments with different $Xklp1_{506}H$ concentrations are shown (top to bottom). In each experiment, asters grew first in the absence of motor (left column), then motor was added (middle column) and removed again (right column). Tubulin concentration was always 30 μM. (B) Inhibition of microtubule shrinkage in the absence of tubulin. Six experiments are shown (top to bottom). After growth of asters either in the absence of motor or in the presence of motor at low concentrations as indicated (left column), tubulin was removed, keeping the motor concentration constant (right column). The requirement of higher motor concentrations for complete inhibition of microtubule dynamics on growing microtubules in the presence of GTP-tubulin can be explained, assuming that free tubulin competes for Xklp1 binding (Fig. 3A). (**C** and **D**) Microtubule asters nucleated from centrosomes and visualized by fluorescence microscopy. (C) Inhibition of microtubule growth by dimeric $Xklp1_{506}H$ and monomeric $Xklp1_{354}H$ in the presence of different adenine nucleotides. Control is without motor. (D) Inhibition of dilution-induced microtubule depolymerization by the two dimeric constructs $Xklp1_{506}H$ and $Xklp1_{507}GST$ and by monomeric $Xklp1_{354}H$ in the presence of ATP. Control is without motor. Bar, 10 μm.

reached their steady-state size and were observed after fixation by fluorescence microscopy (*16*) (Fig. 2C). The inhibition of aster growth by Xklp1$_{506}$H was stronger in the presence of the nonhydrolyzable ATP analog β:γ-imidoadenosine 5′-triphosphate (AMP-PNP) (or in the absence of adenine nucleotide) than in the presence of ATP (or ADP).

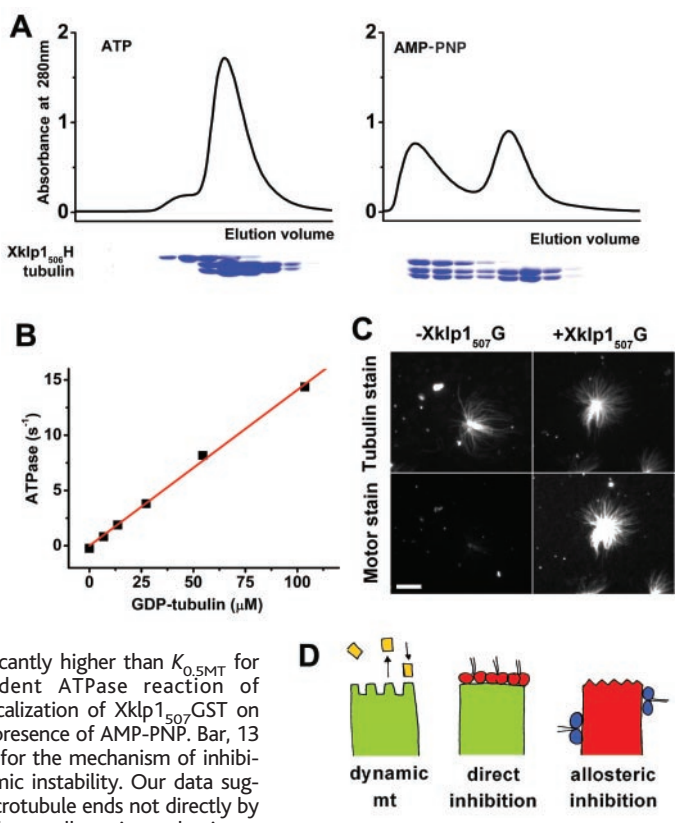

Fig. 3. Xklp1 binds both to dimeric tubulin and to microtubules. (**A**) Gel filtration of Xklp1$_{506}$H in the presence of GDP-tubulin and different adenine nucleotides. Protein elution profiles measured by UV absorbance (top) and Coomassie-stained SDS gels of the collected fractions (bottom). They reveal no binding of motor to tubulin in the presence of ATP and strong binding in the presence of AMP-PNP. (**B**) ATPase activity of Xklp1$_{506}$H stimulated by free GDP tubulin. The nonsaturating increase of the ATPase rate with the high tubulin concentrations used showed that the Michaelis-Menten constant $K_{0.5tubulin}$ was significantly higher than $K_{0.5MT}$ for the microtubule-dependent ATPase reaction of Xklp1$_{506}$H. (**C**) Immunolocalization of Xklp1$_{507}$GST on microtubule asters in the presence of AMP-PNP. Bar, 13 μm. (**D**) Different models for the mechanism of inhibition of microtubule dynamic instability. Our data suggest that Xklp1 affects microtubule ends not directly by forming a cap, but rather by an allosteric mechanism.

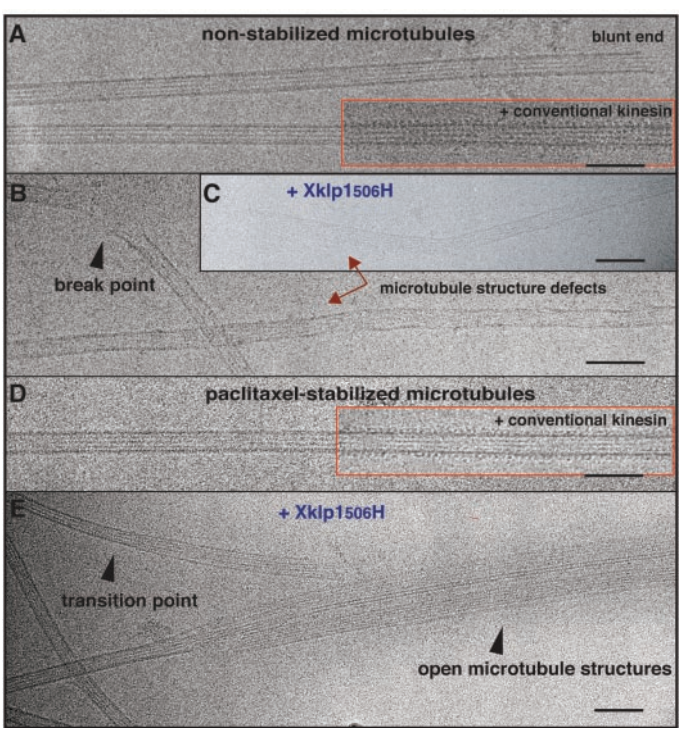

Fig. 4. Effect of Xklp1 on the structure of microtubules visualized by cryo-EM. (**A** to **C**) Microtubules in the absence of paclitaxel: (A) without motor or (inset) with rat kinesin (rK379) (*32*) or (B and C) with substoichiometric amounts of Xklp1$_{506}$H (*16*). Stretches of lattice irregularities or sometimes even break points were induced by Xklp1. (**D** and **E**) Paclitaxel-stabilized microtubules: (D) without motor or (inset) with rat kinesin or (E) with overstoichiometric amounts of Xklp1$_{506}$H (*16*). Microtubules incubated with Xklp1$_{506}$H appeared unraveled and often collapsed to extensive tubulin walls propagating from their ends, as suggested by the parallel appearance of protofilaments, in contrast to the regular alteration of fuzzy and striated (moire) patterns of microtubules without Xklp1. All experiments were performed in the presence of AMP-PNP. Bar, 50 nm.

Thus, the motor-mediated inhibition of microtubule dynamics did not require the hydrolysis of ATP but did correlate with the strength of Xklp1$_{506}$H binding to microtubules (Fig. 1C). Using Xklp1$_{507}$GST and a monomeric construct, Xklp1$_{354}$H (*16*) (fig. S3), as controls, we showed that neither the presence of the His-tag nor dimerization of the motor were necessary for inhibition of microtubule dynamics (Fig. 2, C and D).

Similar to KinI kinesins (*13*, *29*), Xklp1$_{506}$H also bound to free tubulin (Fig. 3A) and possessed ATPase activity stimulated by free tubulin (Fig. 3B) (*16*). However, in contrast to KinI kinesins (*13*, *29*), the steady-state affinity of Xklp1$_{506}$H for microtubules at saturating ATP concentrations was still higher than for free tubulin (compare Fig. 1D and Fig. 3B), and immunolocalization showed no specific binding to microtubule ends (Fig. 3C). Thus, Xklp1's inhibitory effect on microtubule dynamics was probably not due to a direct prevention of loss or gain of tubulin dimers at end structures but rather caused by a change in microtubule structure induced by the presence of bound motor.

To test this hypothesis, we visualized microtubules by cryoelectron microscopy (cryo-EM) after incubation with Xklp1$_{506}$H and AMP-PNP (*16*) under conditions in which Xklp1 induced the majority of the microtubules to be static with rare events of microtubule destabilization (as demonstrated by light microscopy). Cryo-EM revealed microtubules that frequently had defects along the entire lattice, occasionally even showing break points (Fig. 4B) and ends that disintegrated into frayed structures (Fig. 4C). Defects were not observed in control experiments without motor or with dimeric conventional kinesin that fully decorated microtubules (Fig. 4A).

The effect of Xklp1$_{506}$H on the structure of paclitaxel-stabilized microtubules was milder, but also striking. At overstoichiometric ratios of motor, microtubules were unraveled from their predominant supertwisted forms, as indicated by a wider lattice with protofilaments running in parallel. This unwinding, which propagated from the microtubule ends for several hundreds of nanometers, led very often to entirely open and collapsed microtubule walls (Fig. 4E). Partial decoration of Xklp1 was mostly visible along nonperturbed microtubule segments (fig. S4A). Similar results were obtained with monomeric Xklp1$_{354}$H (fig. S4B). Despite the extensive microtubule unraveling, the presence of paclitaxel appeared to inhibit other visible structural defects induced by Xklp1 in nonstabilized microtubules. The extensive unwinding of microtubules was not observed in the absence of Xklp1 or in controls containing constructs of dimeric conventional kinesin (Fig. 4D).

This effect of Xklp1 on the entire microtubule lattice is clearly different from that of destabilizing KinI kinesins that produce microtubule ends from which protofilaments peel off. The structural changes in the microtubule lattice induced by Xklp1 suggest an allosteric mechanism for the inhibition of microtubule dynamic instability (Fig. 3D): Xklp1 bound to the microtubules appears to induce global structural changes in the microtubule lattice that influence the microtubule ends, causing inhibition of microtubule dynamics and, eventually, on a slower time scale, microtubule destabilization.

Bound to chromosome arms in cells (*7*), Xklp1 might contribute to a local decrease of microtubule dynamics. This suggests an extension of the "search and capture" model, which proposes the capture and stabilization of dynamic microtubules exclusively by kinetochores but not by the overall chromosome surface (*30*, *31*). Alternatively, Xklp1 could serve to destabilize microtubules close to chromosomes on a slow time scale. In addition, the motor activity of Xklp1 generates plus end–directed movement that is fast in comparison to the velocity of microtubule polymerization and flux in the spindle, which can explain its proposed role in the extension of spindle poles (*4*). The N-terminal part of Xklp1 containing the motor domain is sufficient for its two activities, motility and inhibition of microtubule dynamic instability.

The motor domain of Xklp1 shares characteristics with two very different classes of kinesin-like proteins: (i) those with a clear transport function like conventional kinesin that undergo ATP-dependent conformational changes upon binding to the microtubule lattice, and (ii) the microtubule-depolymerizing kinesins that cannot translocate along the microtubule lattice in a directed manner, but catalyze ATP hydrolysis when bound to free tubulin. Xklp1 could thus be an evolutionary link between these two classes of kinesins that couple ATP hydrolysis either with motility along the microtubule lattice or with microtubule depolymerization.

References and Notes

1. W. Saunders, V. Lengyel, M. A. Hoyt, *Mol. Biol. Cell* **8**, 1025 (1997).
2. D. J. Sharp, G. C. Rogers, J. M. Scholey, *Nature* **407**, 41 (2000).
3. R. Heald *et al.*, *Nature* **382**, 420 (1996).
4. C. E. Walczak, I. Vernos, T. J. Mitchison, E. Karsenti, R. Heald, *Curr. Biol.* **8**, 903 (1998).
5. D. J. Sharp *et al.*, *J. Cell Biol.* **144**, 125 (1999).
6. X. Yao, A. Abrieu, Y. Zheng, K. F. Sullivan, D. W. Cleveland, *Nature Cell Biol.* **2**, 484 (2000).
7. I. Vernos *et al.*, *Cell* **81**, 117 (1995).
8. H. Funabiki, A. W. Murray, *Cell* **102**, 411 (2000).
9. F. Verde *et al.*, *Nature* **343**, 233 (1990).
10. L. D. Belmont, A. A. Hyman, K. E. Sawin, T. J. Mitchison, *Cell* **62**, 579 (1990).
11. T. Wittmann, A. Hyman, A. Desai, *Nature Cell Biol.* **3**, E28 (2001).
12. K. Kinoshita, I. Arnal, A. Desai, D. N. Drechsel, A. A. Hyman, *Science* **294**, 1340 (2001).
13. A. Desai, S. Verma, T. J. Mitchison, C. E. Walczak, *Cell* **96**, 69 (1999).
14. F. R. Cottingham, L. Gheber, D. L. Miller, M. A. Hoyt, *J. Cell Biol.* **147**, 335 (1999).
15. I. Vernos, unpublished data.
16. Materials and methods are available as supporting material on *Science* Online.
17. J. Howard, *Annu. Rev. Physiol.* **58**, 703 (1996).
18. J. M. Scholey, Ed., *Motility Assays for Motor Proteins*, vol. 39 of *Methods in Cell Biology* (Academic Press, 1993).
19. Y. Sekine *et al.*, *J. Cell Biol.* **127**, 187 (1994).
20. D. D. Hackney, *Nature* **377**, 448 (1995).
21. A. Kallipolitou *et al.*, *EMBO J.* **20**, 6226 (2001).
22. A. Lockhart, R. A. Cross, *Biochemistry* **35**, 2365 (1996).
23. D. D. Hackney, *Biophys. J.* **68**, 267S (1995).
24. T. G. Huang, D. D. Hackney, *J. Biol. Chem.* **269**, 16493 (1994).
25. S. P. Gilbert, T. A. Mackey, *Methods* **22**, 337 (2000).
26. D. D. Hackney, *Annu. Rev. Physiol.* **58**, 731 (1996).
27. J. Howard, *Mechanics of Motor Proteins and the Cytoskeleton* (Sinauer, Sunderland, MA, 2001).
28. S. Leibler, D. A. Huse, *J. Cell Biol.* **121**, 1357 (1993).
29. A. W. Hunter *et al.*, *Mol. Cell* **11**, 445 (2003).
30. T. J. Mitchison, *Annu. Rev. Cell Biol.* **4**, 527 (1988).
31. T. J. Mitchison, M. W. Kirschner, *J. Cell Biol.* **101**, 766 (1985).
32. G. Skiniotis *et al.*, *EMBO J.* **22**, 1518 (2003).

33. We thank M. Utz for technical assistance, N. Mücke (DKFZ, Heidelberg) for help with the analytical ultracentrifugation, G. Tsiavaliaris (Max Planck Institute for Medical Research, Heidelberg) for help with the stopped-flow measurements, A. Hoenger and T. Wendt for help with the cryo-EM, R. Cross (Marie Curie Research Institute, Oxted) for pET17bGST, A. Popov and F. Nédélec for centrosomes, and I. Arnal (CNRS, Rennes) for axonemes. Supported by DFG grant SU 175/4-1. H.B. was supported by the German National Merit Foundation.

Supporting Online Material

www.sciencemag.org/cgi/content/full/303/5663/1519/DC1
Materials and Methods
Figs. S1 to S4
References

17 December 2003; accepted 16 January 2004

A Toll-like Receptor That Prevents Infection by Uropathogenic Bacteria

Dekai Zhang, Guolong Zhang,* Matthew S. Hayden, Matthew B. Greenblatt, Crystal Bussey, Richard A. Flavell, Sankar Ghosh†

Toll-like receptors (TLRs) recognize molecular patterns displayed by microorganisms, and their subsequent activation leads to the transcription of appropriate host-defense genes. Here we report the cloning and characterization of a member of the mammalian TLR family, TLR11, that displays a distinct pattern of expression in macrophages and liver, kidney, and bladder epithelial cells. Cells expressing TLR11 fail to respond to known TLR ligands but instead respond specifically to uropathogenic bacteria. Mice lacking TLR11 are highly susceptible to infection of the kidneys by uropathogenic bacteria, indicating a potentially important role for TLR11 in preventing infection of internal organs of the urogenital system.

TLRs represent a family of transmembrane proteins characterized by multiple copies of leucine-rich repeats in the extracellular domain and a cytoplasmic Toll/IL-1 (interleukin-1) receptor homology domain (TIR) (*1*, *2*). Currently 10 TLRs have been reported in mammalian species, and these appear to recognize distinct pathogen-associated molecular patterns (PAMPs). Of these known TLRs, TLR2, TLR3, TLR4, TLR5, and TLR9 have been extensively characterized (*1*, *2*). TLR1, TLR6, TLR7, and TLR8 have not yet been shown to independently impart signals after recognition of specific microbial products. Heterodimerization between certain TLRs also helps to increase the diversity of PAMPs that can be recognized (*3*, *4*).

The completion of the human and mouse genome sequence has provided the opportunity to determine whether the mammalian TLR family extends beyond the 10 known members. To identify as yet uncharacterized TLRs, we used the sequence of the TIR domain of TLR4 to search National Center for Biotechnology Information (NCBI) databases. The sequence encoding TLR11 was first detected as an expressed-sequence tag (EST) from a mouse liver EST database. Sequential searches using this EST ultimately led to the recovery of the mouse genomic sequence encoding TLR11. The GENSCAN program (*5*) was used to predict the putative open reading frame (ORF), and hypothetical translation predicted a 907 amino acid protein with the hallmarks of known Toll receptors, including a leucine-rich domain, a transmem-

Section of Immunobiology and Department of Molecular Biophysics and Biochemistry, Howard Hughes Medical Institute, Yale University School of Medicine, New Haven, CT 06520, USA.

*Present address: Department of Animal Science, Oklahoma State University, Stillwater, OK 74078, USA.

†To whom correspondence should be addressed: sankar.ghosh@yale.edu.